BIOCHEMISTRY
including biophysical chemistry & molecular biology
Article

*Biochemistry* **2010,** *49,* 9839–9847 9839
DOI: 10.1021/bi101305b

# Glycosaminoglycans of the Porcine Central Nervous System†

Zhenling Liu,‡,§ Sayaka Masuko,§ Kemal Solakyildirim,§ Dennis Pu,§ Robert J. Linhardt,§ and Fuming Zhang*,§

‡*College of Chemistry and Chemical Engineering, State Key Laboratory of Applied Organic Chemistry, Lanzhou University, Lanzhou 730000, P. R. China, and* §*Departments of Chemistry and Chemical Biology, Biology, and Chemical and Biological Engineering, Center for Biotechnology and Interdisciplinary Studies, Rensselaer Polytechnic Institute, 110 8th Street, Troy, New York 12180, United States*

*Received August 14, 2010; Revised Manuscript Received September 22, 2010*

ABSTRACT: Glycosaminoglycans (GAGs) are known to participate in central nervous system processes such as development, cell migration, and neurite outgrowth. In this paper, we report an initial glycomics study of GAGs from the porcine central nervous system. GAGs of the porcine central nervous system, brain and spinal cord were isolated and purified by defatting, proteolysis, anion-exchange chromatography, and methanol precipitation. The isolated GAG content in brain was 5 times higher than in spinal cord (0.35 mg/g of dry sample, compared to 0.07 mg/g of dry sample). In both tissues, chondroitin sulfate (CS) and heparan sulfate (HS) were the major and the minor GAG, respectively. The average molecular masses of CS from brain and spinal cord were 35.5 and 47.1 kDa, respectively, and those for HS from brain and spinal cord were 56.9 and 34 kDa, respectively. The disaccharide analysis showed that the compositions of CS from brain and spinal cords are similar, with uronic acid (1→3) 4-*O*-sulfo-*N*-acetylgalactosamine residue corresponding to the major disaccharide unit (CS type A) along with five minor disaccharide units. The major disaccharides of both brain and spinal cord HS were uronic acid (1→4) *N*-acetylglucosamine and uronic acid (1→4) 6-*O*-sulfo-*N*-sulfoglucosamine, but their composition of minor disaccharides differed. Analysis by $^1$H and two-dimensional NMR spectroscopy confirmed these disaccharide analyses and provided the glucuronic/iduronic acid ratio. Finally, both purified CS and HS were biotinylated and immobilized on BIAcore SA biochips. Interactions between these GAGs and fibroblast growth factors (FGF1 and FGF2) and sonic hedgehog (Shh) were investigated by surface plasmon resonance.

Brain and spinal cord are the two main components of the central nervous system (CNS).[1] The extracellular matrix of the CNS serves as both a supporting structure for cells and a rich source of signaling molecules that can influence cell proliferation, survival, migration, and differentiation (*1*).

Chondroitin sulfate proteoglycans (CSPGs), known to be diffusely present in the CNS matrix and the condensed matrix of perineuronal nets (PNNs) (*2*), are involved in the regulation of neuronal plasticity (*3*, *4*), in neuroprotection (*5*, *6*), and in support of ion homeostasis around highly active neurons (*7*−*9*). The polysaccharide component of CSPGs, the CS GAGs are key to the binding and biological activities of CSPGs, as the result of the positioning of sulfo groups by specific saccharide sequences. There is a growing body of evidence that shows that CS is a uniquely important GAG in morphogenesis, cell division, and cartilage development. CSPGs are spatiotemporally regulated during brain development and upregulated after injury in the CNS. CS is a sulfated GAG composed of a repeating disaccharide backbone of →4) *β*-D-glucuronic acid (GlcA) (1→3) *β*-D-*N*-acetylgalactosamine (GalNAc) (1→ potentially containing some L-iduronic acid (IdoA) residues and *O*-sulfo group substitution. GlcA containing CS can belong to class CS-A (chondroitin 4-sulfate), CS-C (chondroitin 6-sulfate), CS-D (chondroitin 2,4-disulfate), or CS-E (chondroitin 4,6-disulfate). Class CS-B (dermatan sulfate) is comprised of a 4-*O*-sulfo-GalNAc 1→4 linked to IdoA. Nonsulfated (chondroitin) disaccharide can also be found in the CS structure. Studies relying on synthetic approaches using carbohydrate microarrays have demonstrated that CS-E is the principal motif involved in the interaction of CS with midkine, a heparin-binding growth factor involved in neural development (*10*). Chondroitin 4-sulfate (CS-A) also has been shown to negatively regulate axonal guidance and growth (*11*−*15*) (Figure 1).

HS consists of →4) *β*-D-GlcA (or IdoA) (1→4) *β*-D-*N*-acetylglucosamine (GlcNAc) (1→ with various *N*-sulfo and *O*-sufo subtitutions (*16*). HS PGs are ubiquitous in all animal tissues and are also found in brain and nervous tissue. HS PG glypican-2 (cerebroglycan), for example, is uniquely important in the developing nervous system and is expressed predominantly during neuronal differentiation (*17*). HS can mediate repulsion and collapse of olfactory axons (*18*) and is essential for the binding of various growth factors (*19*) and Semaphorin 5A (*20*).

Glycomics research is currently undergoing rapid development as a result of recent advances in technologies for glycan structural

†This work was supported by grants from the National Institutes of Health (GM38060) and the New York State Spinal Cord Injury Program (C022061 to R.J.L.). Z.L. was supported by China Scholarship Council.

*To whom correspondence should be addressed. Phone: (518) 276-6839. Fax: (518) 276-3405. E-mail: zhangf2@rpi.edu.

[1]Abbreviations: CNS, central nervous system; CSPGs, chondroitin sulfate proteoglycans; HS, heparan sulfate; PGs, proteoglycans; CS, chondroitin sulfate; SPR, surface plasmon resonance; FGF, fibroblast growth factor; Shh, sonic hedgehog; GAG, glycosaminoglycan; ECM, extracellular matrix; SA, streptavidin; FC, flow cell; PAGE, polyacrylamide gel electrophoresis; MW, molecular weight; CO, cutoff; GlcA, glucuronic acid; GalNAc, *N*-acetylgalactosamine; IdoA, iduronic acid; GlcNAc, *N*-acetylglucosamine; LC-MS, liquid chromatography and mass spectrometry; NMR, nuclear magnetic resonance; CHAPS, 3-[(3-cholamidopropyl)dimethylammonio]-1-propanesulfonate; RU, resonance unit.


Published on Web 10/18/2010

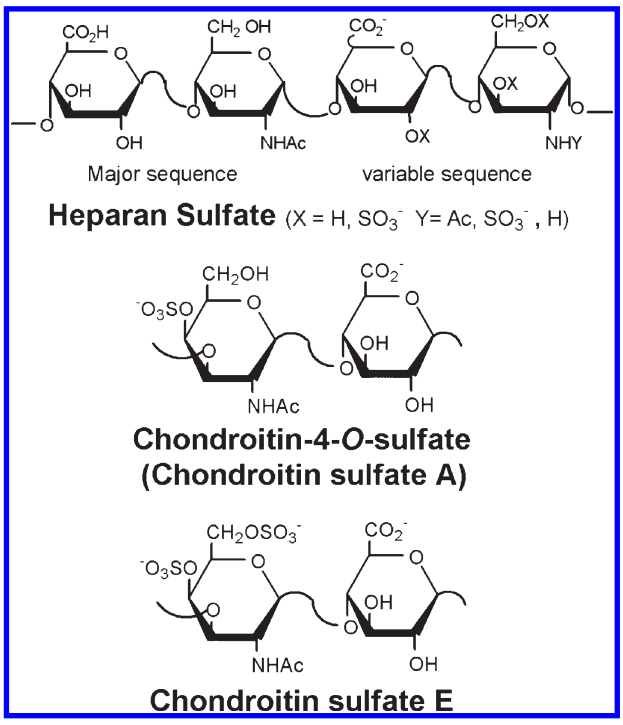


FIGURE 1: Chemical structures of HS, CS-A, and CS-E.

analysis that is beginning to unravel the structure−activity relationships of glycan−protein interactions (*21*). In this paper, we report an initial glycomics study of GAGs from the porcine CNS. CS and HS were isolated from porcine brain and spinal cords, purified, and quantified, and their average molecular weight ($MW_{avg}$) was determined. Disaccharide composition, determined using liquid chromotography and mass spectrometry (LC−MS), and structural analysis relying on $^1H$ and two-dimensional NMR spectroscopy were conducted. These purified CS and HS GAGs were biotinylated and immobilized on BIAcore SA biochips, and their interactions with fibroblast growth factors (FGF1 and FGF2) and sonic hedgehog (Shh) were investigated using surface plasmon resonance (SPR).

## EXPERIMENTAL PROCEDURES

*Materials*. Adult healthy porcine brains (two brains) and spinal cords (four cords) were purchased from Pel-freez Biological Inc. (Rogers, AR). Actinase E was from Kaken Biochemicals (Tokyo, Japan). CS-A (bovine tracheal cartilage) and CS-E (squid cartilage) and chondroitin lyases (ABC and ACII) were from Seikagaku Corp. (Tokyo, Japan). HS (porcine intestine) was from Celsus Laboratories (Cincinnati, OH). Flavobacterial heparin lyases I, II, and III were expressed in *Escherichia coli* and purified in our laboratory. Polyacrylamide, urea, CHAPS, Alcian blue dye, 2-cyanoacetamide, and tetra-*n*-butylammonium hydrogen sulfate were from Sigma (St. Louis, MO).

Unsaturated CS disaccharide standards [Di-0S, ΔUA-GalNAc (where ΔUA is Δ-deoxy-L-*threo*-hex-4-enopyranosyluronic acid); Di-4S, ΔUA-GalNAc4S; Di-6S, ΔUA-GalNAc6S; Di-UA2S, ΔUA2S-GalNAc; Di-di$S_B$, ΔUA2S-GalNAc4S; Di-di$S_D$, ΔUA-2S-GalNAc6S; Di-di$S_E$, ΔUA-GalNAc4S6S; Di-triS, ΔUA2S-GalNAc4S6S] and unsaturated heparin/HS disaccharide standards (Di-0S, ΔUA-GlcNAc; Di-NS, ΔUA-GlcNS; Di-6S, ΔUA-GlcNAc6S; Di-UA2S, ΔUA2S-GlcNAc; Di-UA2SNS, ΔUA2S-GlcNS; Di-NS6S, ΔUA-GlcNS6S; Di-UA2S6S, ΔUA2S-GlcNAc6S; Di-triS, ΔUA2S-GlcNS6S) were obtained from Seikagaku Corp.

Fibroblast growth factor 1 (FGF1) and fibroblast growth factor 2 (FGF2) were gifts from Amgen (Thousands Oaks, CA). Sonic hedgehog (Shh) was generously provided by D. Leahy (Johns Hopkins University, Baltimore, MD).

*Methods*. (*i*) *Isolation and Purification of GAGs*. Porcine brain and spinal cord samples were crushed with dry ice into very fine homogenized powder using a blender (from Fisher Scientific). Fat was removed by washing the tissues with a chloroform/methanol mixture [2:1, 1:1, 1:2 (v/v)] each left overnight. Defatted samples were proteolyzed at 55 °C with 10% actinase E (20 mg/mL) for 18 h. After the proteolysis, dry urea and dry CHAPS were added to each sample (2 wt % in CHAPS and 8 M in urea). The resulting cloudy solutions were clarified by being passed through a syringe filter containing a 0.2 μm membrane from Millipore (Billerica, MA). A Vivapure MAXI Q H spin column was equilibrated with 3 mL of 8 M urea containing 2% CHAPS (pH 8.3). The clarified filtered samples were loaded onto and run through the Vivapure MAXI Q H spin columns (Sartoriou Stedim Biotech, Bohemia, NY) under centrifugal force (500*g*). The columns were first washed with 3 mL of 8 M urea containing 2% CHAPS (pH 8.3). The columns were then washed five times with 5 mL of 200 mM NaCl. GAG was recovered from the spin column after it was washed three times with 1 mL of 16% NaCl; these washes were collected and combined, and methanol (12 mL) was added to afford an 80 vol. % methanol solution that was equilibrated at 4 °C for 18 h, resulting in a precipitate that was recovered by centrifugation (2500*g*) for 30 min. The precipitate was dissolved in 0.5 mL of water, and the recovered total GAGs were stored frozen for further analysis.

(*ii*) *Isolation of CS and HS from the Total GAG Mixture*. GAG samples were digested with a mixture of heparin lyases I, II, and III (10 milliunits each) at 35 °C for 38 h to isolate CS. CS was purified with a Vivapure MINI Q H spin column and centrifugal filtration using a 3000 Da molecular weight cutoff (MWCO) membrane (Millipore, Bedford, MA). HS was recovered by digestion of total GAGs with chondroitinase ABC and chondroitinase ACII (5 milliunits each) at 37 °C for 38 h. The HS products were recovered with the same process as CS. HS was purified with a Vivapure MINI Q H spin column and centrifugal filtration using a 3000 Da MWCO membrane. The total GAGs, CS, and HS were quantified by a carbazole assay (*22*) using CS-A as the standard.

(*iii*) *Polyacrylamide Gel Electrophoresis Analysis*. Polyacrylamide gel electrophoresis (PAGE) was used to determine the $MW_{avg}$ and polydispersity of each GAG sample. In each lane, ~5 μg of total GAG, CS, or HS was subjected to electrophoresis against a standard composed of a mixture of oligosaccharides with known molecular weights that had been prepared enzymatically from bovine lung heparin. The gel was visualized with Alcian blue staining and then digitized with UN-Scan-it (Silk Scientific), and $MW_{avg}$ and polydispersity were calculated (*23*).

(*iv*) *Disaccharide Analysis Using LC−MS*. The GAG substrate (20 μg/μL) was treated with 5 μL of a mixture of 0.1 unit each of chondroitin lyase ABC and chondroitin lyase ACII dissolved in 500 μL of 0.1% BSA and incubated at 37 °C overnight. The products were filtered using 3000 Da MWCO centrifugal filters, and the CS disaccharides were recovered in the filtrate. The disaccharides were freeze-dried, and exactly 100 μL of $H_2O$ was added prior to their analysis. Next, heparin lyase I, II, and III [3 milliunit each in 10 μL of sodium phosphate (5 mM, pH 7.1) buffer] were added to the retentate, and the mixture was incubated at 37 °C overnight. The products were again filtered using 3000 Da

MWCO centrifugal filters, and the HS disaccharides were recovered in the filtrate. The disaccharides were freeze-dried, and exactly 100 $\mu$L of $H_2O$ was added prior to their analysis.

Disaccharide analysis was performed on a LC−MS system (Agilent LC/MSD trap MS). Solutions A and B for the HPLC separation contained 37.5 mM $NH_4HCO_3$ and 11.25 mM tributylamine in 15 and 70% acetonitrile, respectively. The pH values of these solutions were adjusted to 6.5 with acetic acid. Separation was performed on a C-18 column [2.1 mm × 150 mm (Waters, Milford, MA)] at a flow rate of 10 $\mu$L/min using solution A for 20 min, followed by a linear gradient from 20 to 45 min from 0 to 50% solution B. The column effluent entered the source of the ESI-MS for continuous detection by MS. The electrospray interface was set in the negative ionization mode with a skimmer potential of −40.0 V, a capillary exit at −40.0 V, and a source temperature of 325 °C to obtain the maximum abundance of the ions in full scan spectra (150−1500 Da, 10 full scans/s). Nitrogen was used as a drying (5 L/min) and nebulizing gas (20 psi). The CS disaccharide separation was performed on an Acquity UPLC BEH C18 column [2.1 mm × 150 mm, 1.7 $\mu$m (Waters)] using solution A for 10 min, followed by a linear gradient from 10 to 40 min from 0 to 50% solution B. The column temperature was maintained at 45 °C. The flow rate was 100 $\mu$L/min. Solutions A and B for UPLC were 0 and 75% acetonitrile, respectively, containing the same concentration of 15 mM hexylamine (HXA) as an ion pairing reagent and 100 mM 1,1,1,3,3,3-hexafluoro-2-propanol (HFIP) as an organic modifier. We extracted the ions on the basis of their theoretical mass unit, ionization mode, and addition of ion pairing reagent.

(*v*) *NMR Analysis*. Total GAG, CS, and HS isolated from porcine brain and porcine spinal cord were analyzed by $^1$H NMR and two-dimensional NMR (HSQC and HHCOSY) spectroscopy to characterize their structures. All NMR experiments were performed on a Bruker Advance II 600 MHz spectrometer with Topsin version 2.0. Commercial HS and CS-A and samples were each dissolved in 0.5 mL of $D_2O$ [99.996% (Sigma)] and freeze-dried repeatedly to remove the exchangeable protons. The samples were redissolved in 0.3 mL of $D_2O$ and transferred to NMR microtubes [outside diameter of 5 mm (Shigemi)]. The conditions for one-dimensional $^1$H spectra were as follows: wobble sweep width of 12.3 kHz, acquisition time of 2.66 s, and relaxation delay of 8.00 s. The temperature was 298 or 323 K. The conditions for two-dimensional HMQC spectra were as follows: 32 scans, sweep width of 6.15 kHz, acquisition time of 0.33 s, and relaxation delay of 0.90 s. The conditions for two-dimensional COSY spectra were as follows: 16 scans, sweep width of 7.40 kHz, acquisition time of 0.28 s, and relaxation delay of 1.50 s.

(*vi*) *Biotinylation of GAG*. CS and HS (300 $\mu$g) were incubated in a 500 mM NaOH solution at 4 °C for 16 h and then neutralized by gradual addition of glacial acetic acid to cleave the xylose−serine linkage. The products were desalted using a YM-3 spin column. The resulting CS and HS GAG chains (200 $\mu$g) and amine-$PEO_3$-biotin (200 $\mu$g) were dissolved in 100 $\mu$L of $H_2O$, then 10 $\mu$g of $NaCNBH_3$ was added. The reaction mixture was heated at 70 °C for 24 h, and a further 10 mg of $NaCNBH_3$ was added and the mixture heated at 70 °C for an additional 24 h. After cooling to room temperature, the mixture was desalted with a spin column (3000 Da MWCO). Biotinylated GAGs were collected, freeze-dried, and used for SA chip preparation.

(*vii*) *Preparation of the SPR Biochip*. SPR was performed on a BIAcore3000 (GE Healthcare, Uppsala, Sweden). Buffers were filtered (0.22 $\mu$M) and degassed. The biotinylated GAGs were immobilized on flow cells in a streptavidin chip. A flow cell was treated with biotin alone and served as a control. The successful immobilization of GAG was confirmed by the observation of an ~300 resonance unit (RU) increase in the sensor chip. Two chips were prepared: the HS chip immobilized with HS from brain, HS from spinal cord, and commercial HS as a positive control and the CS chip immobilized with CS from brain, CS from spinal cord, and commercial CS-E as a positive control.

(*viii*) *Kinetic Measurements of Protein−GAG Interaction Using SPR*. The protein sample (FGF1, FGF2, and Shh) was diluted in HBS-EP buffer [0.01 M Hepes (pH 7.4), 0.15 M NaCl, 3 mM EDTA, and 0.005% surfactant P20] (GE Healthcare). Different dilutions of protein samples in buffer were injected at a flow rate of 30 $\mu$L/min. At the end of the sample injection (180 s), the same running buffer was passed over the sensor surface to facilitate dissociation for 180 s. After dissociation, the sensor surface was regenerated by injection of 2 M NaCl. The response was monitored as a function of time (sensorgram) at 25 °C. SPR experiments were conducted in duplicate or triplicate at each concentration to confirm the bindings were repeatable. Multi-concentration data were globally fit, and residuals were calculated and used to assess the goodness of fit.

Table 1: Quantification and Average MW Characterization of Isolated GAGs from Porcine Brain and Spinal Cord

| | porcine brain | porcine spinal cords |
|---|---|---|
| wet weight (g) | 75.60 | 313.51 |
| dry weight (g) | 15.15 | 87.54 |
| defatted weight (g) | 4.74 | 12.79 |
| total GAGs isolated (mg) | 5.3 | 6.0 |
| mg of GAGs/g of dry tissue | 0.35 | 0.069 |
| CS/HS ratio | 3.4 | 5.9 |
| average CS $MW_{avg}$ (kDa) | 35.5 | 47.1 |
| average HS $MW_{avg}$ (kDa) | 56.9 | 34 |

## RESULTS

*GAG Purification and Quantification*. A simple four-step procedure involving defatting, protease digestion, strong anion-exchange chromatography on a spin column, and methanol precipitation was used to isolate GAGs from the porcine brain and spinal cord. This method had been previously established in our laboratory for the quantitative isolation of heparin from human plasma (*24*) (Table 1). After being freeze-dried and weighed, the samples were defatted. As expected, both spinal cord and brain showed a high fat content of 85 and 69% [(grams of fat per gram of dry weight) × 100], respectively. The total GAG isolated from each sample was next determined using the carbazole assay for uronic acid. The GAG content of the dry, defatted sample from brain (0.35 mg/g) was 5 times higher than the GAG content of spinal cord (0.07 mg/g). CS and HS were each purified from the total GAG by selective polysaccharide digestion using heparin and chondroitin lyases, respectively. The CS/HS ratio in porcine spinal cord was 5.9 and in porcine brain was 3.4.

*Polyacrylamide Gel Electrophoresis* (*PAGE*) *Analysis* (*see Figure S1 of the Supporting Information for gel pictures*). Total GAGs, CS and HS, isolated from the brain and spinal cord were analyzed by using PAGE with Alcian blue staining. PAGE analysis established that CS and HS were both present in spinal cord and brain and showed a broad band of expected polydispersity

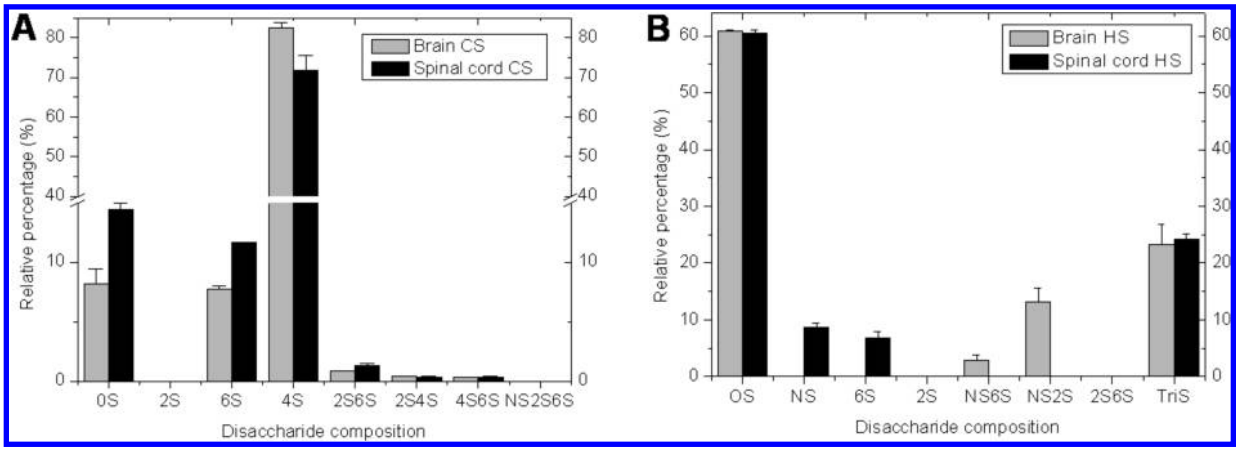


FIGURE 2: Disaccharide compositional analysis of HS and CS from different tissues by LC−ESI-MS. (A) Disaccharide composition of CS from porcine brain and spinal cord. (B) Disaccharide composition of HS from porcine brain and spinal cord. Data represent the average values with the standard error (bar) of triplicate experiments.

and the $MW_{avg}$ (*23*). The $MW_{avg}$ of CS was 35.5 kDa in brain and 47.1 kDa in spinal cord, and the $MW_{avg}$ of HS was 56.9 kDa in brain and 34 kDa in spinal cord.

*Compositional Analysis of GAG Disaccharides*. Compositional analysis of disaccharides gives important structural information and is an efficient method for measuring the variation of GAG structures. HS can contain different disaccharide sequences, including those corresponding to the eight heparin/HS disaccharide standards (see Experimental Procedures for details). Similarly, CS/DS GAGs also can contain different disaccharide sequences, including those corresponding to the eight CS/DS disaccharide standards. An LC−MS analysis method that relies on ion pairing reversed-phase capillary HPLC was used to determine the GAG disaccharide composition (*25*, *26*). This method affords good resolution in the separation of eight heparin/HS or eight CS/DS disaccharides (see Figures S2−S5 of the Supporting Information for MS spectra). CS and HS from porcine brain and spinal cords were first digested with chondroitin lyase ABC and chondroitin lyase AC II or heparin lyases I, II, and III, followed by disaccharide composition analysis using LC−ESI-MS. All peaks are conclusively identified by retention time and via their mass spectra (see Figures S2−S5 of the Supporting Information for MS spectra). The results (Figure 2 A) showed that the major disaccharide of CS was ΔUA-GalNAc4S (> 83 and > 73% in brain and spinal cord, respectively). In addition, ΔUA-GalNAc, ΔUA-GalNAc6S, small amounts of ΔUA2S-GalNAc6S, ΔUA2S-GalNAc4S, and ΔUA4S-GalNAc6S were also observed in CS from both tissues. The major disaccharides of HS (Figure 2 B) from both brain and spinal cord were ΔUA-GlcNAc (~60%) and ΔUA2S-GlcNS6S (~25%). There were some differences in the minor HS disaccharide composition of porcine brain and porcine spinal cord. ΔUA-GlcNS6S and ΔUA2S-GlcNS were found in brain HS, while ΔUA-GlcNS and ΔUA-GlcNAc6S were found in spinal cord HS.

*NMR Spectra*. Because there are no detailed reports about the structural characterization of the GAGs from porcine brain and spinal cord, one-dimensional (1D) NMR analysis and two-dimensional (2D) NMR analysis of the GAGs were performed. $^1$H NMR spectra and 2D NMR (HMQC and COSY) of total GAGs from porcine brain and spinal cord along with $^1$H NMR spectra of CS and HS were obtained (Table 2 and Figures 3 and 4). The majority of the signals present in the $^1$H NMR spectra of the total GAGs isolated from both the brain and spinal cord were present in the $^1$H NMR spectrum of a standard commercial CS-A obtained from bovine tracheal cartilage. The prominent signals include the anomeric protons of GalNAc at 4.478 ppm and of GlcA at 4.393 ppm, H-2 and H-3 of GalNAc at 3.9 ppm, H-3 of GlcA at 3.498 ppm, H-2 of GlcA at 3.285 ppm, and the $CH_3$ of the acetyl group of GalNAc at 2.02 ppm. In addition, the $^1$H NMR spectra of total GAGs showed weak signals at 3.2 ppm and the signals after 5.0 ppm, which are not found in the $^1$H NMR spectra of the CS-A standard. The $^1$H NMR spectrum of standard commercial HS shows prominent signals at 3.19 and 5.00 ppm, the signals of H2 of GlcNS6S and H1 of IdoA of HS, respectively. The ratio of GlcA to IdoA in the total GAG samples from brain and spinal cord is > 10 based on the integration of the intense 4.393 ppm peak for GlcA (in both CS and HS) and the 5.00 ppm peak for IdoA. The ratio of the 4.478 ppm signal for GalNAc, the hexoamine unit in CS, and the 5.38 ppm signal GlcNAc, the hexoamine unit in HS, was 9:1, corresponding closely to the ratio of CS to HS in both tissues that was obtained using the carbazole assay (Table 1). The $^1$H NMR spectra of HS recovered from both the brain and spinal cord were typical of an HS showing a characteristic ratio of D-GlcA to L-IdoA of > 2.0 (*16*). The $^1$H NMR spectra of CS recovered from both the brain and spinal cord contained only GlcA and were typical

Table 2: Proton and Carbon Chemical Shifts of Major GlcUA and GalNAc Residues Present in Chondroitin Sulfate (CS-A)

| | chemical shift ($\delta$, ppm) | |
|---|---|---|
| proton or carbon of CS-A | GlcA | GalNAc |
| H-1 | 4.393 | 4.478 |
| H-2 | 3.285 | 3.946 |
| H-3 | 3.498 | 3.924 |
| H-4 | 3.693 | 4.670 |
| H-5 | 3.627 | 3.754 |
| H-6a | – | 3.711 |
| H-6b | – | 3.711 |
| $CH_3$ | – | 2.02 |
| C-1 | 104.30 | 101.10 |
| C-2 | 72.30 | 51.33 |
| C-3 | 73.83 | 75.79 |
| C-4 | 80.14 | 75.55 |
| C-5 | 76.34 | 74.51 |
| C-6 | – | 61.05 |
| $CH_3$ | – | 22.14 |

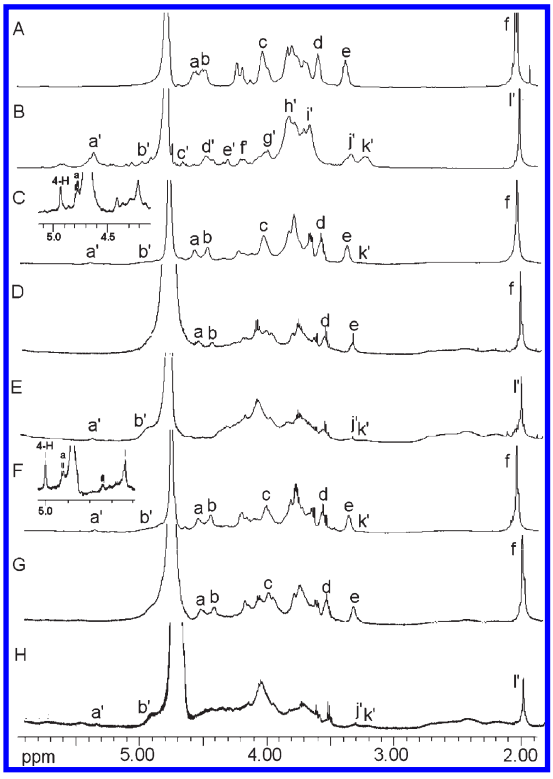


FIGURE 3: $^1$H NMR spectra (600 MHz) of standard CS-A from bovine tracheal cartilage (A), standard heparan sulfate obtained from porcine intestine (B), total GAG from brain (C), CS from brain (D), HS from brain (E), total GAG from spinal cord (F), CS from spinal cord (G), and HS from spinal cord (H) recorded in $D_2O$ at 298 K. Signals: (a) H-1 of GalNAc, (b) H-1 of GlcA, (c) H-2 and H-3 of GalNAc, (d) H-3 of GlcA, (e) H-2 of GlcA, (f) $CH_3$ of the acetyl group of GalNAc, (a′) H-1 of GlcNAc or IdoA2S, (b′) H-1 of IdoA, (c′) H-5 of IdoA2S, (d′) H-1 of GlcA, (e′) H-2 of IdoA2S, (f′) H-3 of IdoA2S and H-6 GlcNS6S or GlcNAc6S, (g′ and h′) H-2 and H-3 of GlcNAc and H-6 and H-5 of GlcNS or GlcNAc, respectively, (i′) H-3 and H-4 of GlcNS, GlcNAc, GlcNS6S, or GlcNAc6S, (j′) H-2 of GlcA, (k′) H-2 of GlcNS or GlcNS6S, and (l′) $CH_3$ of the acetyl group of GlcNAc.

of a CS. $^1$H NMR spectra of total GAG from the two tissues were recorded at an elevated temperature (323 K) to confirm that chondroitin 4-sulfate (CS-A) was the main GAG component in porcine brain and porcine spinal cord (Figure 3, inset). At 323 K, all the signals of GAGs shift downfield by ~0.3 ppm. The strong peak at 5.00 ppm was identified as H-4 of GalNAc4S; this peak overlapped with the HOD signal in the $^1$H NMR spectra at 298 K. The HMQC spectra of total acidic GAGs from brain and spinal cord were also overlaid onto the HMQC spectrum of CS-A (Figure 4). The correlation signals of the CS-A covered all the major peaks present in the HMQC spectra of GAGs from both brain and spinal cord.

*SPR Measurements of the Interaction of Proteins with CS and HS from Porcine Brain and Spinal Cord.* The interactions between the GAGs and proteins from the fibroblast growth factor signaling system (FGF1 and FGF2) and hedgehog signaling pathway (Shh) were investigated using surface plasmon resonance (SPR) to determine the bioactivities of GAGs from two tissues of porcine CNS. The results (Table 3 and Figure 5) showed that brain CS had negligible ($> 1\ \mu$M $K_D$) binding for all proteins except for Shh. Spinal cord HS bound tighter than brain HS to all proteins tested. Brain and spinal cord CS bound Shh ($< 1\ \mu$M $K_D$) even while the more highly charged CS-E failed to interact. Shh showed very slow off rates compared to those determined for FGF1 and FGF2. Spinal cord HS and CS showed very strong binding to FGF1 and FGF2, while brain CS only weakly bound these growth factors.

## DISCUSSION

Over the past few decades, genomics and proteomics have led to high-throughput measurements of expression of several thousand genes and hundreds of protein−protein interactions required for understanding comprehensive biochemical pathways and interaction networks within cells and organisms. Applying the same "omics" concept in glycobiology, or glycomics, requires a multidimensional approach involving isolation, structural characterization, and functional studies of glycans that eventually can lead to important structure−function relationships (*27*). Glycomics necessarily relies on a diverse range of analytical technologies, including MS, NMR, HPLC, CE, SPR, arrays, natural and synthetic glycan libraries, microfluidic systems, bioinformatics, and molecular modeling of glycans. The most extensively studied complex glycans are the GAGs, which involved in many critical biological processes, including development, angiogenesis, anticoagulation, axonal growth, cancer, and microbial/viral pathogenesis.

As part of our interest in the treatment of spinal cord injury with chondroitin lyases (*28*), a class of enzymes extensively studied in our laboratory (*29*), we became interested in the GAGs present in the CNS. Despite research activity in this area, it was surprising to discover how little was known about the GAG content, structure, and protein binding affinities of CNS PGs in adult mammals. Approximately 20% of the volume of the adult CNS is occupied by extracellular matrix (ECM), which is composed primarily of PGs (*30*). The major proteoglycans found in the CNS are members of the lectican family, which have a protein core whose N-terminus binds to hyaluronan (HA) and a middle portion that contains attachment sites for CS GAG chains. It is known that CSPGs are widely expressed in the developing and adult central nervous system (CNS). They have been implicated in regulating cell proliferation, survival, migration, and differentiation. Furthermore, CSPGs are the principal inhibitory component of glial scars, which form after damage to the adult central nervous system and act as a barrier to regenerating axons (*31*). CSPG-mediated inhibition of growth seems to be linked to the activation of several signaling pathways. Thus, the importance of these critical functions of the CSPGs in CNS suggested that we undertake a glycomics study of porcine CNS for which brain and spinal cord tissues are readily available as a model for the human CNS.

This study reveals that the brain has a 5-fold higher GAG content than the spinal cord. CS is the prominent GAG in CNS PGs (both brain and spinal cord), corresponding to 77−86%, with HS being a minor component (14−23%) in total GAG (Table 1). While brain CS had a 30% lower $MW_{avg}$ than spinal cord CS, both exhibited comparable disaccharide analyses (Table 1 and Figure 2). CNS CS is primarily ($> 70\%$) chondroitin 4-sulfate (CS-A) sequences, followed by nearly equal amounts (~10−15% each) of chondroitin and chondroitin 6-sulfate CS-C sequences, and minor amounts ($< 1\%$ each) of disulfated sequences [chondroitin 2,6-sulfate (CS-D), chondroitin 4,6-sulfate (CS-E), and chondroitin 2,4-sulfate]. NMR analysis fails to detect the presence of significant amounts of IdoA, suggesting little if any DS is present in the porcine CNS. The placement of these disaccharides into larger sequence motifs, however, appears to be different, resulting in selective binding critical in CNS

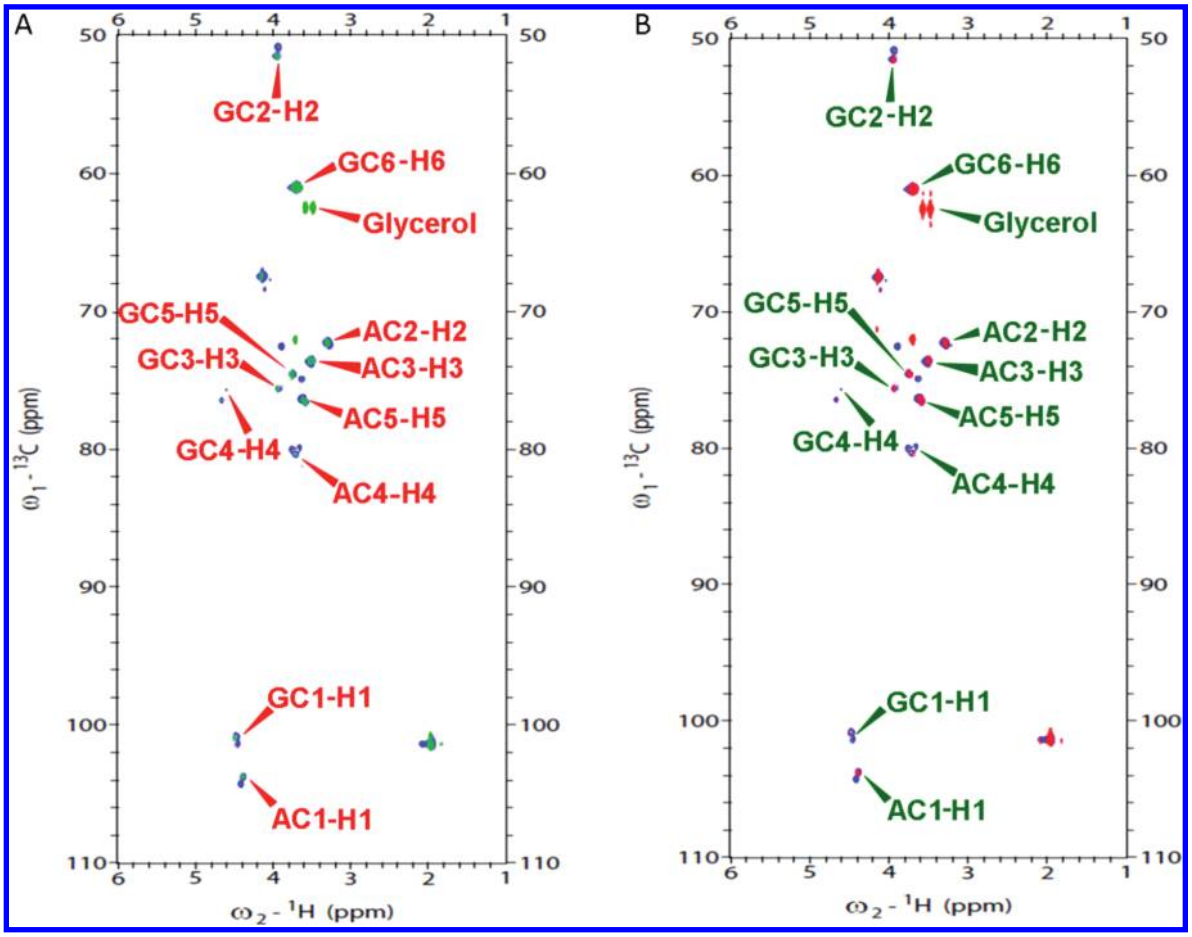


FIGURE 4: $^{1}H-^{13}C$ HMQC spectrum (600 MHz) for total GAG from brain (green) overlaid onto CS-A (blue) (A) and total GAG from spinal cord (red) overlaid onto CS-A (blue) (B) at 298 K. A for GlcA and G for GalNAc.

Table 3: Summary of Kinetic Data of Protein−GAG Interactions

| protein | GAG | $k_{on}$ ($M^{-1}$ $s^{-1}$) | $k_{off}$ ($s^{-1}$) | $K_D$ ($\mu$M) |
|---|---|---|---|---|
| FGF1 | brain CS | not available | not available | not available |
| | spinal cord CS | $1.3 \times 10^6$ | 0.22 | 0.17 |
| | CS-E control | $4.1 \times 10^4$ | 0.28 | 6.9 |
| | brain HS | $4.9 \times 10^5$ | 0.42 | 0.88 |
| | spinal cord HS | $5.0 \times 10^5$ | 0.21 | 0.43 |
| | HS control | $2.0 \times 10^5$ | 0.073 | 0.37 |
| FGF2 | brain CS | $2.0 \times 10^5$ | 0.39 | 2.0 |
| | spinal cord CS | $5.1 \times 10^5$ | 0.13 | 0.24 |
| | CS-E control | $2.2 \times 10^5$ | 0.16 | 0.70 |
| | brain HS | $3.8 \times 10^5$ | 0.23 | 0.62 |
| | spinal cord HS | $5.2 \times 10^5$ | 0.17 | 0.32 |
| | HS control | $9.0 \times 10^6$ | 0.12 | 0.013 |
| Shh | brain CS | $7.2 \times 10^3$ | $4.8 \times 10^{-3}$ | 0.67 |
| | spinal cord CS | $1.1 \times 10^4$ | $4.6 \times 10^{-3}$ | 0.43 |
| | CS-E control | 851 | $2.8 \times 10^{-3}$ | 3.3 |
| | brain HS | $1.1 \times 10^4$ | 0.012 | 1.1 |
| | spinal cord HS | $1.5 \times 10^4$ | 0.014 | 0.95 |
| | HS control | $1.8 \times 10^4$ | 0.015 | 0.84 |

growth and development. Brain CS shows no measurable binding to FGF1 and weak binding to FGF2, while spinal cord CS binds tightly to both growth factors. Interestingly, spinal cord CS binds these FGFs with greater affinity than the more highly sulfated CS-E. Thus, it is clear that while similar in disaccharide composition, brain CS and spinal cord CS exhibit different protein binding affinities, suggesting that the sequence or arrangement of these disaccharides is critical to their biological function.

We next turned our attention to the HS present in the CNS. Brain HS was ~30% larger than spinal cord HS, while both contained nearly identical amounts of two major disaccharides, the expected unsulfated disaccharide (~60%) and the unusual trisulfated disaccharide (~24%), possibly corresponding to low and high sulfate domains associated with HS-based signaling (*32*). In contrast, the contents of monosulfated and disulfated disaccharides in the brain and spinal cord HS were very different, with the brain HS being richer in disulfated disaccharides and the spinal cord HS being richer in monosulfated disaccharides. A comparison of our results, on the HS disaccharide composition of mammalian brain, with those from other investigators demonstrates a relative abundance of the TriS disaccharide (20−25% in porcine brain). This value is considerably higher than the results obtained with bovine brain in our laboratory (*33*) and rat brain by others (*34*, *35*). In these prior publications, the percent TriS was $<5\%$. This unexpectedly high abundance of TriS in the HS from porcine brain and spinal cord tissues might result from the higher recovery of the highly sulfated HS chains compared to the undersulfated HS chains causing an enrichment of HS chains containing TriS during the extraction process. It is noteworthy that the structural differences have been reported for GAGs isolated from different species or different organ systems within given single species and even within the same organ system of a single species at different stages of development.

Differences in either composition or sequence result in a consistent higher binding affinity of spinal cord HS for FGF1, FGF2, and Shh.

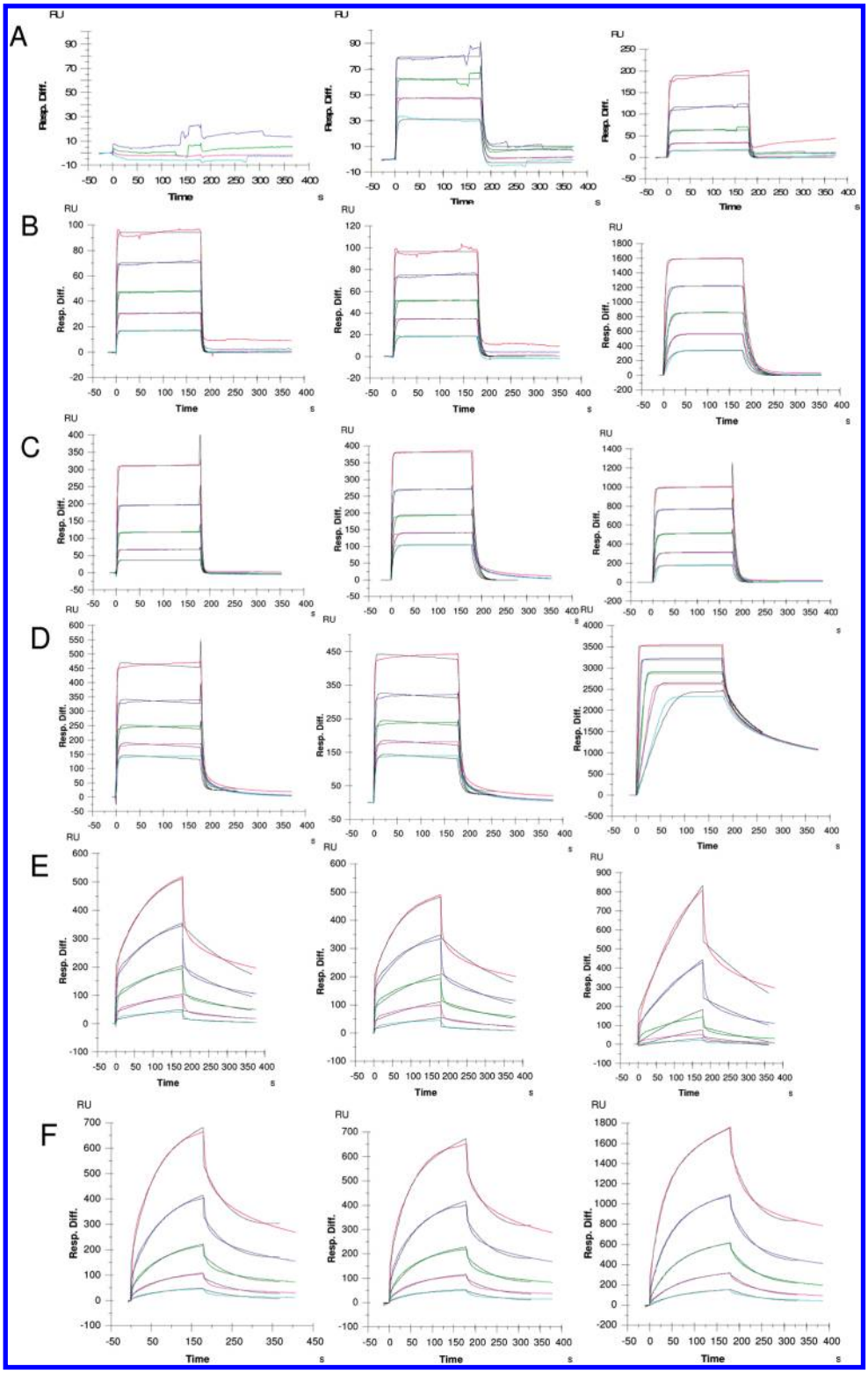


FIGURE 5: Sensorgrams of GAG−protein interactions. Concentrations of proteins: 1000, 500, 250, 125, and 63 nM (from top to bottom, respectively). The black curves in all sensorgrams are the fitting curves using models from BIAevaluate version 4.0.1. (A) SPR sensorgrams of CS−FGF1 interaction: (left) brain CS, (middle) spinal cord CS, and (right) CS-E control. (B) SPR sensorgrams of HS−FGF1 interaction: (left) brain HS, (middle) spinal cord HS, and (right) HS control. (C) SPR sensorgrams of CS−FGF2 interaction: (left) brain CS, (middle) spinal cord CS, and (right) CSE control. (D) SPR sensorgrams of HS−FGF2 interaction: (left) brain HS, (middle) spinal cord HS, and (right) HS control. (E) SPR sensorgrams of CS−Shh interaction: (left) brain CS, (middle) spinal cord CS, and (right) CS-E control. (F) SPR sensorgrams of HS−Shh interaction: (left) brain HS, (middle) spinal cord HS, and (right) HS control.

Extensive studies of the FGF family show their multiple critical roles in the formation of the CNS from the early stage of neural induction through the late stage of terminal differentiation (*36*). FGF1 and FGF2 have been found to be potent modulators of proliferation in the developing nervous system (*37*). Recently, it was reported that FGF1 was a potent neurotrophic factor that affects neuronal survival in the injured spinal cord (*38*). FGF signaling begins with the formation of a ternary

complex of FGF, FGF receptor (FGFR), and HS. HS serves primarily as a template for the assembly of the $FGF_2$−$FGFR_2$−$HS_2$ signal transduction complex (*39*). It is noteworthy that most HS species used to study FGF signaling have been obtained from porcine intestine used in the commercial preparation of heparin; few if any reports have examined the FGF binding of tissue specific GAGs.

Shh is a member of the hedgehog family of signaling molecules identified by homology to *Drosophila* hedgehog. Shh was identified as a morphogen that is directly responsible for dorso-ventral patterning of the CNS. Additional multiple actions of Shh during CNS development have been well established, including the specification of oligodendrocytes, proliferation of neural precursors, and control of axon growth (*40*). Recently, Lowry et al. reported that the transplantation of endothelial-expanded neural stem cells treated with Shh and retinoic acid into an adult mouse spinal cord injury model resulted in significant recovery of sensory and motor function (*41*). In the hedgehog signaling pathway, HSPGs are essential for the proper distribution and signaling activity of signaling proteins (*42*). It is well established that Shh interacts with heparin and HS, and these interactions are important for normal hedgehog signaling (*38*, *43*). Thus, it is interesting that Shh binds both porcine brain and porcine spinal cord CS with higher affinity than HS from the same tissues.

In conclusion, glycosaminoglycans (GAGs) were successfully isolated and purified from the central nervous system (brain and spinal cord). Their molecular structure (i.e., average molecular weight and disaccharide composition) was characterized by PAGE and LC−MS disaccharide analysis, and more detailed structural features were revealed by $^1H$ and two-dimensional NMR spectroscopy. Finally, interactions between these GAGs and proteins [including fibroblast growth factors (FGF1 and FGF2) and sonic hedgehog (Shh)] were investigated by SPR, providing important structure−activity information. The methodology described will be useful in tissue specific glycomics research in discovering novel glycotherapeutics that target disease-related protein−GAG interactions.

## SUPPORTING INFORMATION AVAILABLE

PAGE analysis of GAGs (Figure S1) and MS spectra (Figure S2−S5). This material is available free of charge via the Internet at http://pubs.acs.org.

## REFERENCES


1. Sherman, L. S., and Back, S. A. (2008) A 'GAG' reflex prevents repair of the damaged CNS. *Trends Neurosci. 31*, 44–52.
2. Sarama, S. D., Daniela, C., Clare, G., Kate, R., Junko, F., Tadahisa, M., Kazuyuki, S., and James, W. F. (2006) Composition of Perineuronal Net Extracellular Matrix in Rat Brain, a different disaccharide composition for the net-associated proteoglycans. *J. Biol. Chem. 281*, 17789–17800.
3. Hockfield, S., Kalb, R. G., Zaremba, S., and Fryer, H. (1990) Expression of Neural Proteoglycans Correlates with the Acquisition of Mature Neuronal Properties in the Mammalian Brain. *Cold Spring Harbor Symp. Quant. Biol. 55*, 505–514.
4. Pizzorusso, T., Medini, P., Berardi, N., Chierzi, S., Fawcett, J. W., and Maffei, L. (2002) Reactivation of ocular dominance plasticity in the adult visual cortex. *Science 298*, 1248–1251.
5. Bruckner, G., Hausen, D., Hartig, W., Drlicek, M., Arendt, T., and Brauer, K. (1999) Cortical areas abundant in extracellular matrix chondroitin sulphate proteoglycans are less affected by cytoskeletal changes in Alzheimer's disease. *Neuroscience 92*, 791–805.
6. Morawski, M., Bruckner, M. K., Riederer, P., Bruckner, G., and Arendt, T. (2004) Perineuronal nets potentially protect against oxidative stress. *Exp. Neurol. 188*, 309–315.
7. Bruckner, G., Brauer, K., Hartig, W., Wolff, J. R., Rickmann, M. J., Derouiche, A., Delpech, B., Girard, N., Oertel, W. H., and Reichenbach, A. (1993) Perineuronal nets provide a polyanionic, glia-associated form of microenvironment around certain neurons in many parts of the rat brain. *Glia 8*, 183–200.
8. Bruckner, G., Hartig, W., Kacza, J., Seeger, J., Welt, K., and Brauer, K. (1996) Extracellular matrix organization in various regions of rat brain grey matter. *J. Neurocytol. 25*, 333–346.
9. Hartig, W., Derouiche, A., Welt, K., Brauer, K., Grosche, J., Mader, M., Reichenbach, A., and Bruckner, G. (1999) Cortical neurons immunoreactive for the potassium channel Kv3.1b subunit are predominantly surrounded by perineuronal nets presumed as a buffering system for cations. *Brain Res. 842*, 15–29.
10. Gama, C. I., Tully, S. E., Sotogaku, N., Clark, P. M., Rawat, M., Vaidehi, N., Goddard, W. A., Nishi, A., III, and Hsieh-Wilson, L. C. (2006) Sulfation patterns of glycosaminoglycans encode molecular recognition and activity. *Nat. Chem. Biol. 2*, 467–473.
11. Hwang, H. Y., Olson, S. K., Esko, J. D., and Horvitz, H. R. (2003) *Caenorhabditis elegans* early embryogenesis and vulval morphogenesis require chondroitin biosynthesis. *Nature 423*, 439–443.
12. Wang, H., Katagiri, Y., McCann, T. E., Unsworth, E., Goldsmith, P., Yu, Z. X., Fei, T., Santiago, L., Mills, E. M., Wang, Y., Symes, A. J., and Geller, H. M. (2008) Chondroitin-4-sulfation negatively regulates axonal guidance and growth. *J. Cell Sci. 121*, 3083–3091.
13. Laabs, T., Carulli, D., Geller, H. M., and Fawcett, J. W. (2005) Chondroitin sulfate proteoglycans in neural development and regeneration. *Curr. Opin. Neurobiol. 15*, 116–120.
14. Sirko, S., von Holst, A., Wizenmann, A., Gotz, M., and Faissner, A. (2007) Chondroitin sulfate glycosaminoglycans control proliferation, radial glia cell differentiation and neurogenesis in neural stem/progenitor cells. *Development 134*, 2727–2738.
15. Silver, J., and Miller, J. H. (2004) Regeneration beyond the glial scar. *Nat. Rev. Neurosci. 5*, 146–156.
16. Toida, T., Yoshida, H., Toyoda, H., Koshiishi, I., Imanari, T., Hileman, R. E., Fromm, J. R., and Linhardt, R. J. (1997) Structural differences and the presence of unsubstituted amino groups in heparan sulphates from different tissues and species. *Biochem. J. 322*, 499–506.
17. Stipp, C. S., Litwack, E. D., and Lander, A. D. (1994) Cerebroglycan: An integral membrane heparan sulfate proteoglycan that is unique to the developing nervous system and expressed specifically during neuronal differentiation. *J. Cell Biol. 124*, 149–160.
18. Hu, H. (2001) Cell-surface heparan sulfate is involved in the repulsive guidance activities of Slit2 protein. *Nat. Neurosci. 4*, 695–701.
19. Kreuger, J., Jemth, P., Sanders-Lindberg, E., Eliahu, L., Ron, D., Basilico, C., Salmivirta, M., and Lindahl, U. (2005) Fibroblast growth factors share binding sites in heparan sulphate. *Biochem. J. 389*, 145–150.
20. Kantor, D. B., Chivatakarn, O., Peer, K. L., Oster, S. F., Inatani, M., Hansen, M. J., Flanagan, J. G., Yamaguchi, Y., Sretavan, D. W., Giger, R. J., and Kolodkin, A. L. (2004) Semaphorin 5A is a Bifunctional Axon Guidance Cue Regulated by Heparan and Chondroitin Sulfate Proteoglycans. *Neuron 44*, 961–975.
21. Turnbull, J. E., and Field, R. A. (2007) Emerging glycomics technologies. *Nat. Chem. Biol. 3*, 74–77.
22. Bitter, T., and Muir, H. M. (1962) A modiWed uronic acid carbazole reaction. *Anal. Biochem. 4*, 330–334.
23. Edens, R. E., Al-Hakim, A., Weiler, J. M., Rethwisch, D. G., Fareed, J., and Linhardt, R. J. (1992) Gradient polyacrylamide gel electrophoresis for determination of the molecular weights of heparin preparations and low-molecular-weight heparin derivatives. *J. Pharm. Sci. 81*, 823–827.
24. Zhang, F., Sun, P., Munoz, E., Chi, L., Sakai, S., Toida, T., Zhang, H., Mousa, S., and Linhardt, R. J. (2006) Microscale Isolation and Analysis of Heparin from Plasma using an Anion Exchange Spin Column. *Anal. Biochem. 353*, 284–286.
25. Thanawiroon, C., Rice, K. G., Toida, T., and Linhardt, R. J. (2004) Liquid Chromatography/Mass Spectrometry Sequencing Approach for Highly Sulfated Heparin-derived Oligosaccharides. *J. Biol. Chem. 279*, 2608–2615.
26. Solakyildirim, K., Zhang, Z. Q., and Linhardt, R. J. (2010) Ultra-performance liquid chromatography with electrospray ion trap mass spectrometry for chondroitin disaccharide analysis. *Anal. Biochem. 397*, 24–28.
27. Sasisekharan, R., Raman, R., and Prabhakar, V. (2006) Glycomics Approach to Structure-Function Relationships of Glycosaminoglycans. *Annu. Rev. Biomed. Eng. 8*, 181–231.
28. Bradbury, E. J., Moon, L. D., Popat, R. J., King, V. R., Bennett, G. S., Patel, P. N., Fawcett, J. W., and McMahon, S. B. (2002) Chondroitinase ABC promotes functional recovery after spinal cord injury. *Nature 416*, 636–640.

29. Zhang, Z., Park, Y., Kemp, M., Zhao, W., Im, A., Shaya, D., Cygler, M., Kim, Y., and Linhardt, R. J. (2009) Liquid chromatography-mass spectrometry to study chondroitin lyase action pattern. *Anal. Biochem. 385*, 57–64.
30. Nicholson, C., and Sykova, E. (1998) Extracellular space structure revealed by diffusion analysis. *Trends Neurosci. 21*, 207–221.
31. Busch, S. A., and Silver, J. (2007) The role of extracellular matrix in CNS regeneration. *Curr. Opin. Neurobiol. 17*, 120–127.
32. Gallagher, J. T., Turnbull, J. E., and Lyon, M. (1992) Patterns of sulphation in heparan sulphate: Polymorphism based on a common structural theme. *Int. J. Biochem. 24*, 553–560.
33. Zhang, Z., Xie, J., Liu, H., Liu, J., and Linhardt, R. J. (2009) Quantification of heparan sulfate disaccharides using ion-pairing reversed-phase microflow high-performance liquid chromatography with electrospray ionization trap mass spectrometry. *Anal. Chem. 81*, 4349–4355.
34. Shi, X., and Zaia, J. (2009) Organ-specific heparan sulfate structural phenotypes. *J. Biol. Chem. 284*, 11806–11814.
35. Deepa, S. S., Carulli, D., Galtrey, C., Rhodes, K., Fukuda, J., Mikami, T., Sugahara, K., and Fawcett, J. W. (2006) Composition of Perineuronal Net Extracellular Matrix in Rat Brain: A different disaccharide composition for the net-associated proteoglycans. *J. Biol. Chem. 281*, 17789–17800.
36. Vaccarino, F. M., Schwartz, M. L., Raballo, R., Rhee, J., and Lyn-Cook, R. (1999) Fibroblast growth factor signaling regulates growth and morphogenesis at multiple steps during brain development. *Curr. Top. Dev. Biol. 46*, 179–200.
37. Ford-Perriss, M., Abud, H., and Murphy, M. (2001) Fibroblast growth factors in the developing central nervous system. *Clin. Exp. Pharmacol. Physiol. 28*, 493–503.
38. Tsai, M.-C., Shen, L.-F., Kuo, H.-S., Cheng, H., and Chak, K.-F. (2008) Involvement of Acidic Fibroblast Growth Factor in Spinal Cord Injury Repair Processes Revealed by a Proteomics Approach. *Mol. Cell. Proteomics 7*, 1668–1687.
39. Zhang, F., McLellan, J. S., Ayala, A. M., Leahy, D. J., and Linhardt, R. J. (2007) Kinetic and structural studies on interactions between heparin or heparan sulfate and proteins of the hedgehog signaling pathway. *Biochemistry 46*, 3933–3941.
40. Martí, E., and Bovolenta, P. (2002) Sonic hedgehog in CNS development: One signal, multiple outputs. *Trends Neurosci. 25*, 89–96.
41. Lowry, N., Goderie, S. K., Adamo, M., Lederman, P., Charniga, C., Gill, J., Silver, J., and Temple, S. (2008) Multipotent embryonic spinal cord stem cells expanded by endothelial factors and Shh/RA promote functional recovery after spinal cord injury. *Exp. Neurol. 209*, 510–522.
42. Ingham, P. W., and McMahon, A. P. (2001) Hedgehog signaling in animal development: Paradigms and principles. *Genes Dev. 15*, 3059–3087.
43. McLellan, J. S., Yao, S., Zheng, X., Geisbrecht, B. V., Ghirlando, R., Beachy, P. A., and Leahy, D. J. (2006) Structure of a heparin-dependent complex of hedgehog and Ihog. *Proc. Natl. Acad. Sci. U.S.A. 103*, 17208–17213.